PASJ: Publ. Astron. Soc. Japan **58**, 951–956, 2006 December 25
© 2006. Astronomical Society of Japan.

MOIRCS Deep Survey. I: DRG Number Counts

Masaru KAJISAWA,[1] Masahiro KONISHI,[2,3] Ryuji SUZUKI,[3] Chihiro TOKOKU,[3]
Yuka KATSUNO UCHIMOTO,[4] Tomohiro YOSHIKAWA,[2,3] Masayuki AKIYAMA,[3] Takashi ICHIKAWA,[2]
Masami OUCHI,[5*] Koji OMATA,[3] Ichi TANAKA,[3] Tetsuo NISHIMURA,[3] Toru YAMADA[3]
[1]*National Astronomical Observatory of Japan, Mitaka, Tokyo 181-8588*
kajisawa@optik.mtk.nao.ac.jp
[2]*Astronomical Institute, Tohoku University, Aramaki, Aoba, Sendai 980-8578*
[3]*Subaru Telescope, National Astronomical Observatory of Japan, 650 North A'ohoku Place, Hilo, HI 96720, USA*
[4]*Institute of Astronomy, The University of Tokyo, Mitaka, Tokyo 181-0015*
[5]*Space Telescope Science Institute, 3700 San Martin Drive, Baltimore, MD 21218, USA*

(Received 2006 September 1; accepted 2006 October 11)

Abstract

We used very deep near-infrared imaging data taken with the Multi-Object InfraRed Camera and Spectrograph (MOIRCS) on the Subaru Telescope to investigate the number counts of Distant Red Galaxies (DRGs). We observed a $4' \times 7'$ field in the Great Observatories Origins Deep Survey-North (GOODS-N), and our data reached $J = 24.6$ and $K = 23.2$ (5σ, Vega magnitude). The surface density of DRGs selected by $J - K > 2.3$ is $2.35 \pm 0.31\,\mathrm{arcmin}^{-2}$ at $K < 22$ and $3.54 \pm 0.38\,\mathrm{arcmin}^{-2}$ at $K < 23$, respectively. These values are consistent with those in the GOODS-South and FIRES. Our deep and wide data suggest that the number counts of DRGs turn over at $K \sim 22$, and the surface density of the faint DRGs with $K > 22$ is smaller than that expected from the number counts at the brighter magnitude. The result indicates that while there are many bright galaxies at $2 < z < 4$ with the relatively old stellar population and/or heavy dust extinction, the number of faint galaxies with a similar red color is relatively small. Different behavior patterns of the number counts of the DRGs and bluer galaxies with $2 < z_{\mathrm{phot}} < 4$ at $K > 22$ suggest that the mass-dependent color distribution, where most of the low-mass galaxies are blue, while more massive galaxies tend to have redder colors, had already been established at that epoch.

Key words: galaxies: evolution — galaxies: high-redshift — infrared: galaxies

1. Introduction

The Distant Red Galaxies (DRGs) are selected in the near-infrared (NIR) wavelength by the simple criterion $J - K > 2.3$ in order to sample high-redshift ($z \gtrsim 2$) galaxies with a significant fraction of evolved stars, such as normal galaxies seen in the present universe, which are often missed by the "drop-out" selection technique for the Lyman break galaxies (Franx et al. 2003). These red $J - K$ colors are produced by a Balmer/4000 Å-break at $2 \lesssim z \lesssim 4$ (the breaks enter between J and K-bands) and/or heavy dust extinction at a similar redshift. In fact, several DRGs have been confirmed to be at $2 < z < 4$ by spectroscopy (van Dokkum et al. 2003; Reddy et al. 2005), and their photometric redshift also lies in the range of $2 \lesssim z \lesssim 4$ (Förster Schreiber et al. 2004).

Several studies found that many DRGs have high star-formation rates (van Dokkum et al. 2004; Knudsen et al. 2005; Reddy et al. 2005), while some of them seem to have only little star-formation activity and evolve passively (Labbé et al. 2005; Papovich et al. 2006). Analyses of the spectral energy distributions (SEDs) suggest that DRGs are more massive ($M_* \gtrsim 10^{11}\,M_\odot$) and older ($\sim$ 1–3 Gyr old) than the UV-bright LBGs at similar redshifts (Förster Schreiber et al. 2004; Iwata et al. 2005; Labbé et al. 2005; Papovich et al. 2006; Kriek et al. 2006). Recently, strong angular clustering of these galaxies has also been reported (Grazian et al. 2006; Foucaud et al. 2006; Quadri et al. 2006).

However, most of these previous studies have focused on the bright (massive) part of DRGs. It is important to sample fainter DRGs and to investigate their properties in order to understand the formation and evolution of more "normal" galaxies. Galaxies with a luminosity of L^* or sub-L^* at $z \sim 3$ would have a K-band magnitude of $K \sim 22$–23. Such very deep NIR data have been limited to relatively small areas so far (e.g., Maihara et al. 2001; Labbé et al. 2003; Minowa et al. 2005).

In the present work, we used very deep and wide NIR data taken with MOIRCS on the Subaru Telescope in order to investigate the number counts of DRGs down to $K = 23$. The wide field of view of MOIRCS ($4' \times 7'$) and the large collecting area of the telescope allowed us to analyze DRGs to a faint magnitude with high statistical accuracy.

The Vega-referred magnitude system is used throughout the paper.

2. Observation and Data Analysis

We performed JHK_s-bands imaging observations of a part of the Great Observatories Origins Deep Survey North (GOODS-N) field with the Multi-Object InfraRed Camera and the Spectrograph (MOIRCS, Ichikawa et al. 2006) on-board the Subaru Telescope on 2006 April 4–9,18 and May 10–11,18–19. MOIRCS has a field of view of about $4' \times 7'$ with $0.''117$ pixel

* Hubble Fellow.

scale. We observed one field of view of MOIRCS centered on $12^h36^m46^s.62$, $+62°13'15''.6$ (J2000), which included the original Hubble Deep Field North (HDF-N, Williams et al. 1996). Here, we use the high-quality J and K_s-band data sets, which include only those frames with a seeing size smaller than $0''.5$ (FWHM). The corresponding exposure times were 5.0 hours in the J-band and 7.7 hours in the K_s-band.

The data were reduced in a standard way using the IRAF software package. At first, the self-skyflat frame was made and used for flat-fielding. We then performed sky subtraction, and co-registered and combined the data. The details of the data processing and the data quality will be described in M. Konishi et al. (in preparation). The FWHMs of the PSFs of the combined images are $0''.42$ in the J-band and $0''.40$ in the K_s-band, and the K_s-band image was convolved with a Gaussian kernel to match the PSF to that in the J-band. FS 23 and FS 27 in the UKIRT faint standard stars were used for flux calibrations in the J and K-bands. We excluded the edges of images with lower sensitivities, and our final multi-band combined images have a slightly smaller field of view of about 24.3 arcmin^2.

Source detection was performed in the K_s-band image using the SExtractor image analysis package (Bertin, Arnouts 1996). We adopted MAG_AUTO from the SExtractor as the total K-band magnitudes of the detected objects. For the color measurements, we used a fixed aperture with an $0''.85$ diameter ($2 \times$ seeing size), and the same apertures were used for the J and K-bands.

The $5\,\sigma$ limiting magnitude at $0''.85$ diameter is about $J = 24.6$ and $K = 23.2$, respectively. We estimated the $1\,\sigma$ background fluctuation in each band by directly measuring the sky fluxes with $0''.85$ apertures randomly placed on the images. The estimated background fluctuations were used to calculate the photometric errors for the detected objects. We performed simulations using the IRAF/ARTDATA package to quantify the detection completeness in the K-band. Our source detection is nearly complete for the point source to $K \sim 23$, and the completeness is 90% at $K \sim 23.3$. We also tested the sensitivity to false detections by running SExtractor on an inverted K_s-band image. Only 15 spurious objects were extracted at $K < 23$, while 1596 objects with $K < 23$ were detected in the normal image.

3. Results

3.1. Selection of DRGs

Figure 1 shows $J - K$ vs K color–magnitude diagram of the objects in the MOIRCS deep imaging field. We selected DRGs based on the criterion $J - K > 2.3$. These DRGs are plotted as the large circles, while the others are shown as the small crosses. The squares show the objects that were identified as point sources in the publicly available GOODS HST/ACS z-band data (Giavalisco et al. 2004). The sequence of these objects is seen at $J - K \lesssim 0.9$, which is consistent with the expected locus of the galactic stars. This suggests that the flux calibration of our data is good enough for selecting DRGs. The $2\,\sigma$ limit at the J-band and the completeness limit at the K-band are also shown (dashed line and dotted-dash line). The deep J-band data (the $2\,\sigma$ limit of $J = 25.6$) allow us to sample those objects with $J - K > 2.3$ down to $K \sim 23.3$.

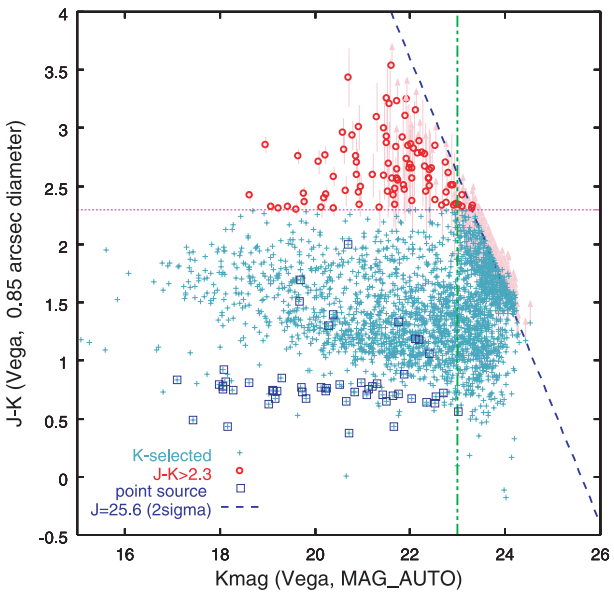

Fig. 1. Color–magnitude diagram of objects in the MOIRCS deep imaging field in the GOODS-North. Galaxies with $J - K > 2.3$ are plotted by large circles. The vertical dotted-dash line represents the completeness limit at the K-band. The dashed line shows the $2\,\sigma$ limit at the J-band. For objects with J-band fluxes lower than the limit, the lower limits of $J - K$ color are plotted by symbols with arrows. Those objects do not necessarily lie on the dashed line because the aperture sizes for the $J - K$ color and the K-band magnitude are different ($0''.85$ diameter and the Kron aperture, respectively). Squares indicates the objects that are identified as point sources in the publicly available GOODS HST/ACS z-band data.

Table 1. Number density of DRGs in the MOIRCS deep field.

K magnitude	Number	Density (arcmin^{-2} mag^{-1})
< 18.5	0	0
18.5–19.0	2	0.16 ± 0.12
19.0–19.5	3	0.25 ± 0.14
19.5–20.0	4	0.33 ± 0.16
20.0–20.5	7	0.58 ± 0.22
20.5–21.0	12	1.07 ± 0.30
21.0–21.5	5	0.41 ± 0.18
21.5–22.0	24	1.98 ± 0.40
22.0–22.5	18	1.48 ± 0.35
22.5–23.0	11	0.91 ± 0.27
K-band limit	Number	Cumulative density (arcmin^{-2})
< 21.0	28	1.15 ± 0.22
< 22.0	57	2.35 ± 0.31
< 23.0	86	3.54 ± 0.38

91 (86 at $K < 23$) DRGs were detected in our field of ~ 24.3 arcmin^2. The cumulative surface density of DRGs down to $K = 21$, 22, 23 is tabulated in table 1. The errors of the surface densities are based on Poisson statistics. The surface density of 1.15 ± 0.22 arcmin^{-2} at $K < 21$ is consistent with those in the HDF-South (HDF-S) and MS 1054−03 field reported by Förster Schreiber et al. (2004).

3.2. Number Counts of DRGs

Figure 2 shows the number counts of the DRGs in the MOIRCS deep imaging field. We show the number counts of all K-selected objects and the DRGs in the top panel. The K-band detection completeness mentioned in the previous section is also plotted. Our data are nearly complete down to $K = 23$, and the number counts in figure 2 are not corrected for the detection completeness. We also show the K-band number counts in other general fields from the literature. The number counts of all K-selected objects in our data are consistent with those in other fields down to $K = 23$.

The number of detected DRGs and their surface density in each K-band magnitude bin are also shown in table 1. The interesting result in figure 2 is that the number counts of DRGs turn over at $K \sim 22$, while the K-band number counts continue to increase to at least $K = 23$, which corresponds to the completeness limit.

In the bottom panel of figure 2, we compare the number counts of DRGs in our data with those in other fields (HDF-S, MS 1054−03, GOODS-South). The HDF-S data by the FIRES survey (Labbé et al. 2003) have a smaller area ($\sim 4.5\,\mathrm{arcmin}^2$), but reach to a deeper completeness limit ($K \sim 23.8$) than our data. The areas of the GOODS-S and MS 1054−03 fields are comparable with, or wider than, this study (~ 130 and $\sim 25\,\mathrm{arcmin}^2$, respectively), but these data reach to a shallower limit of $K \sim 21.5$–22.

Though these four independent fields have different areas and depths, the number counts of DRGs in these fields agree well at $K < 22$. At $K > 22$, only the HDF-S data have a sufficient depth, and can be used for a comparison with our data. The number counts of DRGs in the HDF-S do not show a decrease at $K > 22$, but are still consistent with our results within the uncertainty (see also the next section).

In order to demonstrate the turnover of the DRG counts or the deficit of the faint DRGs relative to the brighter ones, we performed a linear fitting for the number counts of DRGs at $18.5 < K < 22$ using the data in all four fields. The linear fitting at $18.5 < K < 22$ seems to be reasonable because Foucaud et al. (2006) reported that a break feature of the DRG counts lies at $K \sim 18$, and data over $18.5 < K < 22$ of all four fields were fitted well with the linear line. The result is plotted as the dashed line in figure 2. We also tried to fit the MOIRCS data at $K < 22$ by the Maximum Likelihood method without binning the data, and confirmed a very similar result as that of the fitted slope. Thus, the uncertainty due to binning of the data does not affect the fitting result, even if there is a bin with relatively low counts ($K = 21$–21.5 bin).

When we extrapolated this linear line to $K \sim 23$, the surface density of the faint DRGs with $22 < K < 23$ in our field was clearly deficient. The density in the $22.5 < K < 23$ bin is about a factor of three lower than the extrapolation results from the number counts at a brighter magnitude. When we performed a similar linear fitting for the MOIRCS data over $18.5 < K < 23$ with the Maximum-Likelihood method, the fitted slope became 0.19 ± 0.04, which is significantly flatter than the value for the fitting at $18.5 < K < 22$ (0.33 ± 0.07). It is seen that even in the HDF-S, the number of faint DRGs is lower than the extrapolation from the number counts at $K < 22$.

4. Discussion

In this section, we discuss the turnover of the number counts of DRGs at $K \sim 22$ found in the previous section.

At first, we consider the possible spurious effects that could cause a deficit of the faint DRGs. One possibility is that the MAG_AUTO would systematically underestimate the total flux in the K-band near the detection limit (e.g., Labbé et al. 2003); this could cause an underestimation of number of faint DRGs. The number counts of DRGs, however, begins to decrease at $K \sim 22$, which is one magnitude brighter than the *completeness* limit in the K-band, which does not seem to be the case. For example, Labbé et al. (2003) showed that such an underestimation occurs at $K \sim 24$, which is about 0.3 mag fainter than the completeness limit in their FIRES data. Our simulation also indicates that a significant underestimation of the K-band flux does not exist down to at least $K = 23$ (M. Konishi et al. in preparation). In fact, the K-band number counts continues to increase to $K = 23$ in figure 2. We also confirmed that the size distribution of DRGs with $K \sim 23$ is not significantly different from that of the bluer objects. Therefore, there is no reason to think that only DRGs are less complete at $K \sim 23$.

Since most DRGs in our data are resolved, the completeness problems could be more severe than those for the point source. Therefore, we also checked the detection completeness for extended objects. We fitted the K-band surface brightness of relatively bright DRGs with $K < 21$ with the Moffat function, and found that the average FWHM is about $0\farcs58$. Using this surface-brightness profile (assuming the same profile for the fainter DRGs), we performed a similar simulation with that for the point source to quantify the detection completeness as a function of the K-band magnitude. The result is shown in the bottom panel of figure 2 (dotted line). The completeness is more than 90% at $K < 22.5$ and is still 80% at $K = 23$. The detection incompleteness in the K-band cannot explain the observed deficit of the faint DRGs.

A second possibility is that the larger error in the $J - K$ color at a faint magnitude affects the sampling of DRGs. Although the depth of our J-band data (the 2σ limit of $J = 25.6$) is sufficient to sample those objects with $J - K > 2.3$ to $K = 23$, some fraction of the faint DRGs could be missed due to a photometric error. However, we conclude that the error in $J - K$ does not cause any deficit of the faint DRGs, since a similar effect of contamination from bluer objects to the DRG sample also exists. As discussed in Foucaud et al. (2006), since the overall $J - K$ distribution of objects has a peak at a color substantially bluer than $J - K \sim 2.3$, and the objects with $J - K > 2.3$ are relatively rare (figure 1), it can be expected that the number density of DRGs is rather boosted at fainter magnitudes. Therefore, these photometric errors do not seem to cause the observed deficit of DRGs at $K > 22$.

Although the number counts of DRGs in the HDF-S do not show any turnover at $K \sim 22$, as noted in the previous section, the difference in the number density of DRGs at $K > 22$ between that in the HDF-S and that in our MOIRCS field can be explained by the field-to-field variance, when the strong clustering of DRGs is taken into account (e.g., Grazian et al. 2006; Quadri et al. 2006). Grazian et al. (2006) pointed out a large discrepancy of the number density of DRGs with

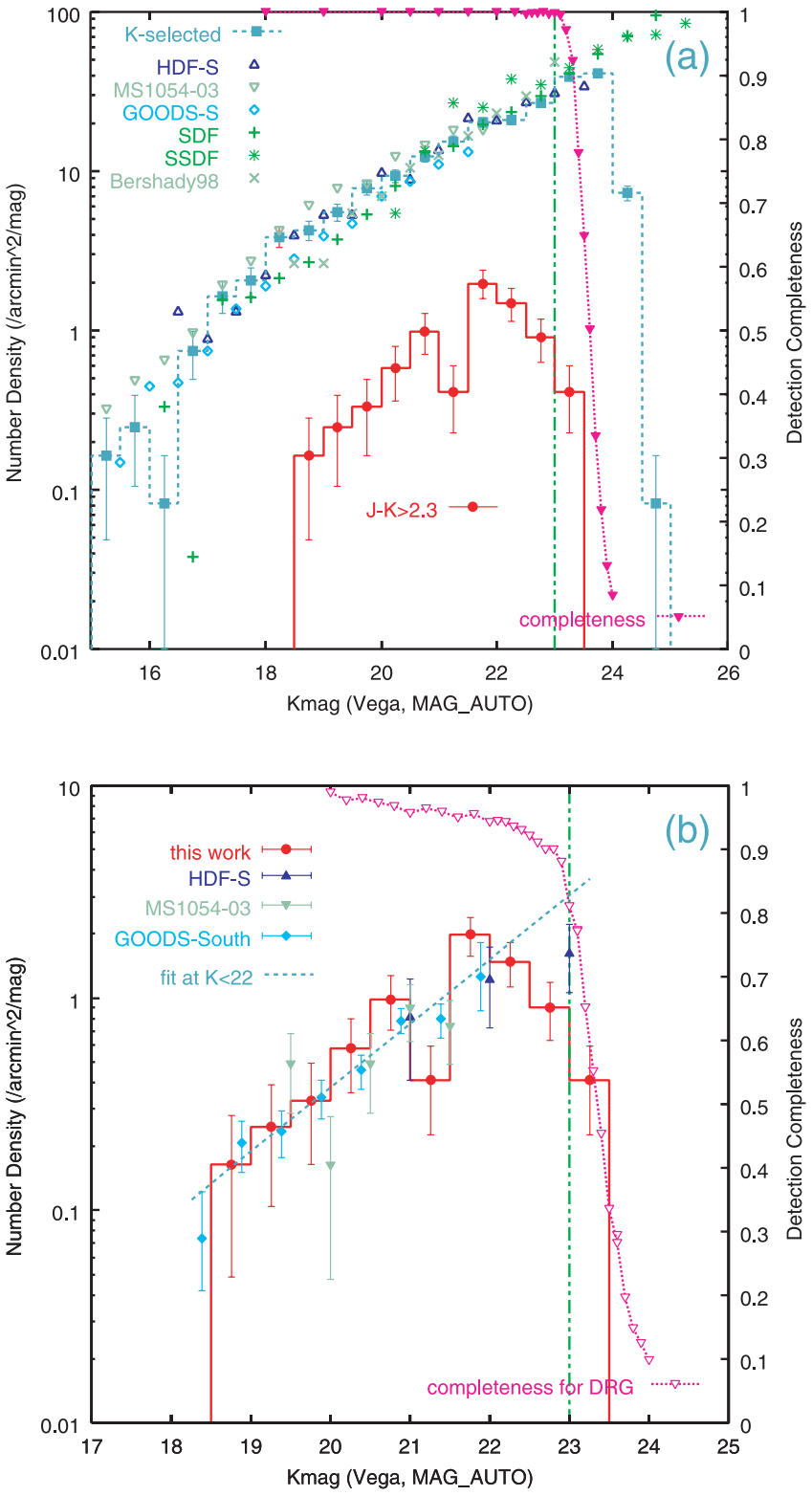

Fig. 2. (a) Number counts of all K-selected objects (squares) and DRGs (circles) in the MOIRCS deep imaging field. The detection completeness in the K-band is also shown (dotted line). The vertical dotted-dash line shows our completeness limit. The K-band number counts in other fields are also shown [HDF-South from Labbé et al. (2003), MS 1054−03 field from Förster Schreiber et al. (2006), GOODS-South from Grazian et al. (2006), Subaru Deep Field from Maihara et al. (2001), Subaru Super Deep Field from Minowa et al. (2005), high galactic latitude fields from Bershady et al. (1998)]. (b) Comparison of DRG number counts. The DRG number counts in other fields are also shown (HDF-South, MS 1054−03, GOODS-South). The dashed line shows a linear fit for the data points at $K < 22$ in all four fields (this study, HDF-S, MS 1054−03, GOODS-S). Errorbars are based on Poisson distribution (i.e., square roots of the observed numbers). The dotted line shows the detection completeness for extended objects with FWHM = 0.″58 (see text).

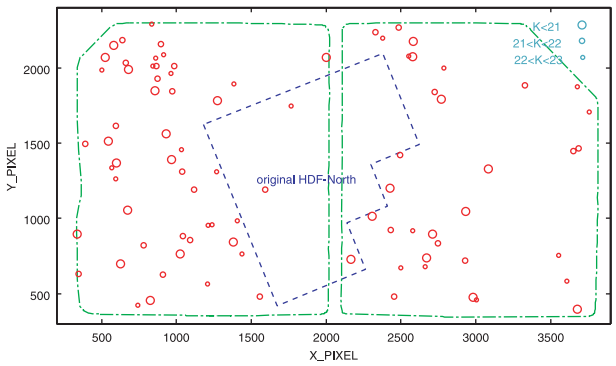

Fig. 3. Spatial distribution of the DRGs. The size of the symbols is scaled according to apparent magnitudes in the K-band (the bigger, the brighter). The dashed line shows the region of the original HDF-N. Dotted-dash lines show the field of view of the MOIRCS data. MOIRCS achieves the field of view of $4' \times 7'$ with two HAWAII-2 arrays. The present version of the combined data was separately reduced for each array, and the deep portion of the field of view was divided into two areas. Two corners (upper left and upper right) were vignetted at the Cassegrain focus of the telescope.

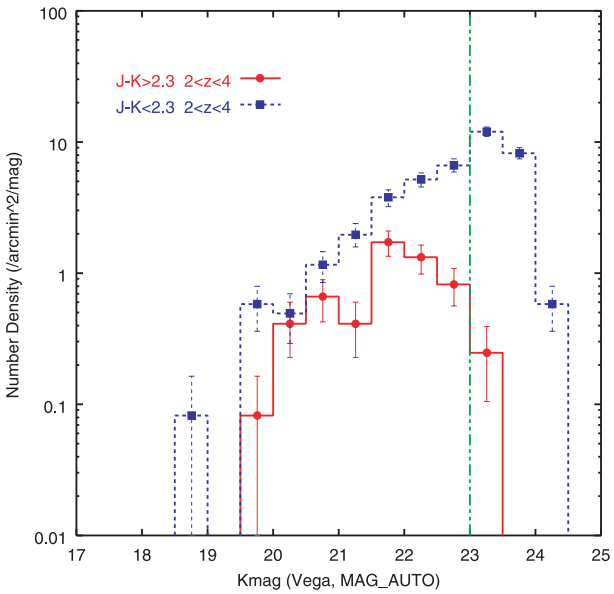

Fig. 4. K-band number counts of galaxies with $2 < z_{\rm phot} < 4$ in the MOIRCS deep imaging field. Circles show those galaxies with $J-K > 2.3$ (i.e., DRGs) and squares represent those with $J-K < 2.3$. Errorbars are based on Poisson distribution. The completeness limit is also shown (dotted-dash line).

$K \lesssim 22$ between the HDF-S and HDF-N (e.g., Dickinson et al. 2000; Fontana et al. 2000). They reported that only two DRGs (one at $K < 21$, one at $21 < K < 22$) exist in the HDF-N, while many DRGs are found in the HDF-S. This can be seen in our data. In figure 3, we plot the spatial distribution of DRGs in the MOIRCS deep field. The region of the original HDF-N is also shown, and there are only two DRGs with $K < 22$ and one DRG with $22 < K < 23$ in this region. On the other hand, there are many DRGs over wide range of K-band magnitude outside of the HDF-N region; not only the bright DRGs, but also the faint ones with $22 < K < 23$ appear to show relatively strong clustering. Such a spatial distribution of DRGs indicates that the small survey areas of the HDFs could introduce large uncertainty, and that a wide area survey is essential for estimating the number density of these galaxies. We will present a detailed analysis of the clustering property of these galaxies in T. Ichikawa et al.'s papers (in preparation).

What does the deficit of faint DRGs at $K > 22$ mean? Previous studies found that most DRGs exist at $2 < z < 4$ (van Dokkum et al. 2003; Reddy et al. 2005; Förster Schreiber et al. 2004). Our photometric redshift estimation with the HST/ACS and MOIRCS data also suggests a similar redshift distribution; 69 out of 86 DRGs with photometric redshift (those detected in more than two bands) have $2 < z_{\rm phot} < 4$ (M. Konishi et al. in preparation). Keeping in mind that some significant fraction of bright DRGs have been confirmed to be at $z < 2$ (e.g., Daddi et al. 2004; Conselice et al. 2006), and that the reliability of the photometric redshift for faint DRGs has not yet been confirmed by spectroscopy, we assume that most DRGs in our data lie at $2 < z < 4$ in the following discussion.

The observed color of $J-K = 2.3$ roughly corresponds to the rest-frame $U-V \sim 0.4$ ($U-B \sim -0.1$) at $2 < z < 4$, which is similar to those of Sc–Sd galaxies seen in the present universe. Such a red color for high-z objects (about 2–3 Gyr age of the universe at $2 < z < 4$) is considered to be produced by a Balmer/4000 Å-break of a relatively old stellar population and/or heavy dust extinction, as mentioned in section 1. Therefore, the turnover of the number counts of DRGs indicates that while there are many bright (massive) galaxies with an old population and/or dusty star-formation activity, the number of the faint galaxies with a similar red color is relatively small at that epoch. Labbé et al. (2005) investigated the stellar mass and SED of DRGs and LBGs with $K < 22$, and found that DRGs dominate the high-mass end at $z \sim 3$. On the other hand, our result from the wide and deep data could suggest that the low-mass end is dominated by galaxies with blue colors, which do not satisfy the criterion of DRG. In figure 4, we show the K-band number counts of galaxies with $2 < z_{\rm phot} < 4$ for DRGs ($J-K > 2.3$) and those with $J-K < 2.3$, separately. It is seen that the fraction of those with $J-K < 2.3$ increases with decreasing K-band flux at $K \gtrsim 22$, while the number density of DRGs is comparable to that of the bluer objects at $K \sim 20$–21. Kajisawa and Yamada (2005, 2006) showed that most low-mass galaxies have a blue rest-frame $U-V$ color, and that the more massive galaxies tend to have a redder color, even at $z \sim 2.5$. Kajisawa and Yamada (2006) also evaluated that the transition mass between these red and blue populations is about $6 \times 10^{10}\,M_\odot$ at $z \sim 2.5$, and in fact most galaxies with $M_* \lesssim 10^{10}\,M_\odot$ have a rather blue color of $U-V \lesssim 0.1$ (their figure 2). Since the magnitude of $K = 22$ of galaxies with $J-K \sim 2.3$ corresponds to about 1–$6 \times 10^{10}\,M_\odot$ at $2 < z < 4$ [we calculated the stellar mass as in Kajisawa and Yamada (2006), using the GALAXEV population synthesis model of Bruzual and Charlot (2003)], the deficit of DRGs at $K > 22$ could be explained by such a mass-dependent color distribution, if a similar trend continues to $z \sim 4$.

We plan to perform a statistical analysis of the SEDs of these galaxies over a wide range of luminosity (and mass) in order to constrain their physical properties in a forthcoming paper.

We would like to thank the Subaru Telescope staff for their in valuable assistance. We would also like to thank Dr. Masato Onodera for useful discussions and an anonymous referee for in valuable comments. M.A.'s activity is supported by a Grant-in-Aid for scientific research from JSPS (18740118). This study is based on data collected at Subaru Telescope, which is operated by the National Astronomical Observatory of Japan. A data reduction/analysis was carried out on "sb" computer system operated by the Astronomical Data Analysis Center (ADAC) and Subaru Telescope of the National Astronomical Observatory of Japan. The Image Reduction and Analysis Facility (IRAF) is distributed by the US National Optical Astronomy Observatories, which are operated by the Association of Universities for Research in Astronomy, Inc., under cooperative agreement with the US National Science Foundation.

References

Bershady, M. A., Lowenthal, J. D., & Koo, D. C. 1998, ApJ, 505, 50
Bertin, E., & Arnouts, S. 1996, A&AS, 117, 393
Bruzual, G., & Charlot, S. 2003, MNRAS, 344, 1000
Conselice, C. J., et al. 2006, ApJ in press (astro-ph/0607242)
Daddi, E., Cimatti, A., Renzini, A., Fontana, A., Mignoli, M., Pozzetti, L., Tozzi, P., & Zamorani, G. 2004, ApJ, 617, 746
Dickinson, M., et al. 2000, ApJ, 531, 624
Fontana, A., D'Odorico, S., Poli, F., Giallongo, E., Arnouts, S., Cristiani, S., Moorwood, A., & Saracco, P. 2000, AJ, 120, 2206
Förster Schreiber, N. M., et al. 2004, ApJ, 616, 40
Förster Schreiber, N. M., et al. 2006, AJ, 131, 1891
Foucaud, S., et al. 2006, MNRAS submitted (astro-ph/0606386)
Franx, M., et al. 2003, ApJ, 587, L79
Giavalisco, M., et al. 2004, ApJ, 600, L93
Grazian, A., et al. 2006, A&A, 453, 507
Ichikawa, T., et al. 2006, Proc. SPIE, 6269, 626916
Iwata, I., Inoue, A. K., & Burgarella, D. 2005, A&A, 440, 881
Kajisawa, M., & Yamada, T. 2005, ApJ, 618, 91
Kajisawa, M., & Yamada, T. 2006, ApJ, 650, 12
Knudsen, K. K., et al. 2005, ApJ, 632, L9
Kriek, M., et al. 2006, ApJ, 645, 44
Labbé, I., et al. 2003, AJ, 125, 1107
Labbé, I., et al. 2005, ApJ, 624, L81
Maihara, T., et al. 2001, PASJ, 53, 25
Minowa, Y., et al. 2005, ApJ, 629, 29
Papovich, C., et al. 2006, ApJ, 640, 92
Quadri, R., et al. 2006, ApJ submitted (astro-ph/0606330)
Reddy, N. A., Erb, D. K., Steidel, C. C., Shapley, A. E., Adelberger, K. L., & Pettini, M. 2005, ApJ, 633, 748
van Dokkum, P. G., et al. 2003, ApJ, 587, L83
van Dokkum, P. G., et al. 2004, ApJ, 611, 703
Williams, R. E., et al. 1996, AJ, 112, 1335